JOURNAL OF OPTOELECTRONICS AND ADVANCED MATERIALS Vol. 10, No. 1, January 2008, p. 98 - 103

Single frequency coherent-population-trapping resonances for magnetic field measurement

S. GATEVA*, E. ALIPIEVA, L. PETROV, E. TASKOVA, G. TODOROV
Institute of Electronics, Bulgarian Academy of Sciences, 72 Tzarigradsko Chaussee, 1784 Sofia, Bulgaria

Experimental investigation of the width, amplitude and shape of the Coherent Population Trapping (CPT) resonances for magnetic field measurements by means of a Hanle effect configuration (the single frequency CPT resonances) is presented. Different resonance width narrowing effects for increasing the sensitivity of the magnetometers are discussed. Numerical simulations based on density matrix formalism, which take into account the influence of the high rank polarization moments and the velocity distribution of the atoms have been performed for analysis of the shapes of the resonances.

(Received September 25, 2007; accepted January 10, 2008)

Keywords: Coherent population trapping, Line shapes and line widths, High rank polarization moments, Magnetometry

1. Introduction

There has been increasing interest in investigation of magnetometers based on magneto-optical effects because they have high sensitivity - comparable to, or even surpassing this of the SQUIDs (Superconducting Quantum Interference Devices) [1] and they can be made smaller and not so expensive as SQUIDs [2]. These magnetometers are appropriate for geomagnetic, space, nuclear and biological magnetic field measurements, environmental monitoring, magnetic microscopy, investigations of fundamental physics, etc. Recent review works on magneto-optics are [3-5].

Coherent population trapping (CPT) resonances, prepared and registered in different ways have been investigated during the last years because they have many applications in high-resolution spectroscopy, magnetometry, lasing without inversion, laser cooling, ultraslow group velocity propagation of light, etc. [6,7]. CPT is observed in three-level atomic systems. Most frequently, two hyperfine levels of the ground state of alkali atoms are coupled to a common excited level. When the frequency difference between the two coupling laser fields equals the frequency difference between the two ground states, the atoms are prepared in a non-absorbing state, which can be registered as a fluorescence quenching and transparency enhancement in spectral interval narrower than the natural width of the observed optical transition [6,8].

CPT resonances can be obtained in a degenerate two-level system, too. In this case, the coherent non-absorbing state is prepared on two Zeeman sublevels of one hyperfine level by monochromatic laser field, and that is why it is called single frequency CPT. Degenerate two-level systems provide further possibilities for the analysis of coherent effects and are important for performing significantly simplified experiments and for building practical devices as well.

For applications, where narrow signals and high signal-to-noise ratios are important, ensuring reliable operation requires good knowledge of the internal and external factors influencing the resonance shape.

In this paper, the single frequency CPT resonance is investigated in uncoated room temperature vacuum cell from point of view of magnetic field measurements. The investigation of the CPT resonance has shown that the resonance has a complex shape - a very narrow (about 1 mG) structure superimposed on a broader one (about few tens of mG). The power dependence of the shapes, amplitudes and widths of the two resonance structures are measured. The observed resonance width narrowing effects are discussed. Numerical simulations based on density matrix formalism, which take into account the high rank polarization moments (HRPM) influence and the velocity distribution of the atoms have been performed for analysis of the shapes of the resonances. The resonances have been investigated at high laser power density in detail.

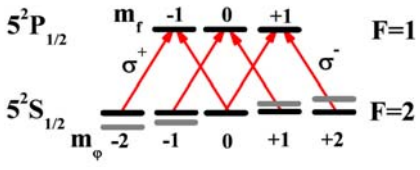

Fig. 1. The ^{87}Rb D_1 line $F_\varphi=2 - F_f=1$ levels connected with linear polarized light.

All investigations were performed on the degenerate two-level system of the ($F_\varphi=2 - F_f=1$) transition of the ^{87}Rb D_1 line by means of a Hanle effect configuration (Fig. 1) because the D_1 line consists of hyperfine transitions at which only dark resonances can be observed, the fluorescence of the $F_\varphi=2 - F_f=1$ transition is practically not overlapping with another and it has the highest contrast (55%) [9].

2. Experimental set up

The experimental set-up is shown in Fig. 2. The resonances were examined in uncoated vacuum cells containing a natural mixture of Rb isotopes at room temperature (20 C). A single-frequency linearly polarized diode laser beam propagating along the cell's axis **x** was used. Its frequency and emission spectrum were controlled by observing fluorescence from a second Rb vapor cell and a F-P spectrum analyzer. A magnetic field $\boldsymbol{B}_{scan}$, created by a solenoid, was applied collinearly to the laser beam. As the shape of the CPT resonance is very sensitive to stray magnetic fields [10,11], the gas cell and the solenoid were placed in a μ-metal magnetic shield. The fluorescence was detected at 90° to the laser beam direction by a photodiode. It was placed close to the front window of the cell because the CPT resonances registered in fluorescence are sensitive to the position of the photodiode along the cell [12]. The transmitted light was detected by a photodiode at the end of the cell. The signals from the photodiodes were amplified and stored in a PC, which also controlled the magnetic field scan. The main sources of errors were the accuracy of the laser power measurements and the poor signal-to-noise ratio at low laser powers.

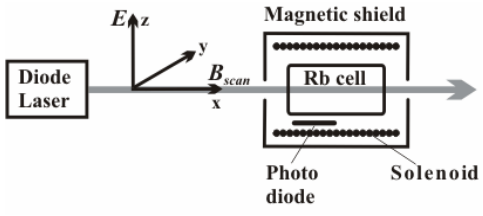

Fig. 2. The experimental setup.

3. Experimental results

3.1. Narrow and wide structure of the CPT resonance

A typical experimental curve is presented in Fig. 3. The CPT resonance has a complex structure. It consists of two parts: a narrow structure (1.7 kHz), centered at zero magnetic field, and superimposed on a broader one (about few tens of mG).

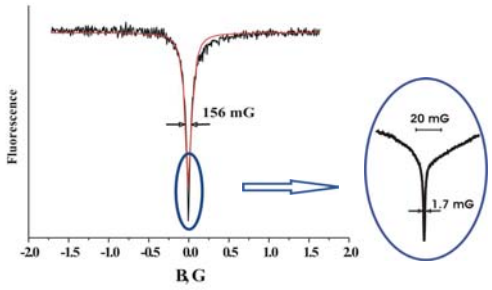

Fig. 3. Dependence of the resonance fluorescence on the magnetic field at laser power density 300 mW/cm² [10].

The detailed investigation of the narrow structure is presented in [10]. In order to obtain information about the processes leading to the narrow structure formation, we performed measurement of its parameters in dependence on the laser power density, additional constant magnetic fields, and the laser frequency position relative to the center of the Doppler broadened line profile. The resonances measured in Rb cells with different dimensions were compared. Evaluation of the influence of different relaxation processes was performed. All these investigations have shown that the origin of the narrow structure is connected with processes in the vacuum cell. The width of the narrow structure of the CPT is in agreement with the assumption that the broadening is mainly affected by the relaxation processes due to atomic collisions with the walls of the cell. The measurements of the resonance width with expanded beam confirm this assumption. The width (FWHM) of the narrow structure $\delta\upsilon$ is determined by $\delta\upsilon = 1/2\pi\tau$, where $\tau = 4V/Sv$, v is the mean thermal velocity, V is the volume and S is the surface area of the cell [13].

3.2. Power dependence of the CPT resonance

Fig. 4 shows the amplitudes of the narrow and the wide structures of the CPT resonance measured as a function of the laser power density. The amplitudes of both signals increase with power. The amplitude of the wide structure increases fast with the power and at intensities larger than 150 mW/cm² saturates. The amplitude of the narrow structure is lower and does not saturate up to a power density of 1 W/cm².

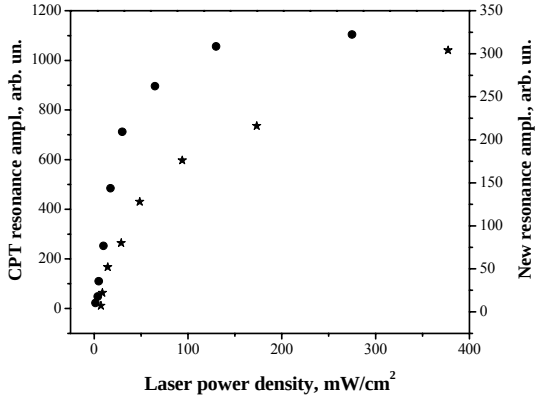

Fig 4. Amplitudes of the narrow (∗) and wide (●) structure of the CPT resonance in dependence on the laser power density.

The narrow structure width does not depend on the laser power, while the wide structure width does - at low powers it increases, and than decreases (Fig. 5). In fluorescence, at laser power densities higher than 1 mW/cm², there is no power broadening, but a resonance-line narrowing with the power - an exponential decrease to ≈80 mG. A possible explanation of this narrowing in our

experiment is the high pumping rate. The CPT signal width is proportional to the pumping rate Ω^2/γ^* (γ^* is the total decay rate of the excited state defined not only by the spontaneous decay but by all relaxation processes) [14]. When the laser power density is increased, the saturation of the absorption cannot be neglected, the decay rate of the excited state γ^* increases due to the stimulated emission and a resonance width narrowing is observed.

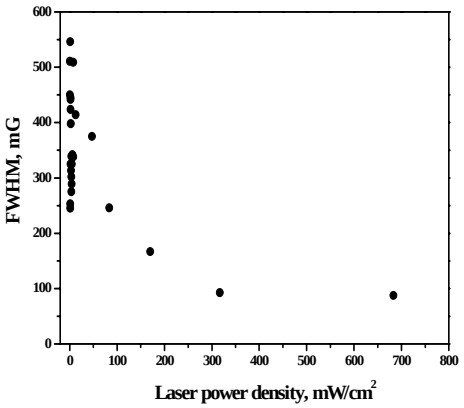

Fig. 5. The width of the wide structure dependence on the laser power density.

The comparison of the narrow structure registered in fluorescence and transmission [15] show that the narrow structure width is the same in fluorescence and transmission and does not depend on the position of the detector. In fluorescence, the narrow resonances can be observed in the whole range of laser powers, while in transmission, in a very small range of powers because of the absorption saturation.

From the point of view of applications in magnetometry, where narrow signals and high signal-to-noise ratios are important, the narrow structure of the CPT resonance measured in fluorescence offers the best possibilities: it is not power broadened; its width does not depend on the position of the detector and its amplitude increases with the power. In the cases when the amplitude of the narrow structure in the CPT resonances is small, the wide structure of the CPT resonance at high laser power densities can be used.

4. Theoretical analysis of the shapes of the CPT resonances

CPT is a nonlinear effect and when the laser power density (the resonance excitation) is increased, together with the transfer of the quadrupole coherence from the ground to excited state, the influence of the multiphoton interactions will increase and high order (high rank) coherences will be created.

Our theoretical investigation of the influence of the high order coherences on the CPT signals was based on the system of equations [16,17] for the density matrix tensor components $\rho_{MM'}$, describing interaction of a degenerate two-level (φ - lower, f – upper level) atomic system with a scanned magnetic field $\boldsymbol{B}_{scan}$, and a resonant, polarized laser field $\boldsymbol{E}(\omega_0,t)$. In irreducible representation this components are related to the polarization moments (PMs) ρ_q^k of rank k ($k = 0,1\ldots 2F_\rho$, $q = M - M'$, where F_ρ is the total angular momentum of the corresponding level, M and M' denote the magnetic sublevels). According to [17] a decomposition of the density matrix in (M, M') representation into tensor components ρ_q^k $q = -k \ldots k$ is described as:

$$\rho_q^k = (2F_\rho + 1)^{1/2} \sum_{M,M'=-F_\rho}^{F_\rho} (-1)^{F_\rho - M} \begin{pmatrix} F_\rho & k & F_\rho \\ -M & q & M' \end{pmatrix} \rho_{MM'} \qquad (1)$$

The parentheses denote the Wigner 3j-symbol.

Besides the clear physical meaning of the tensor components (ρ_0^0 describes the population; ρ_q^1, the orientation and ρ_q^2, the alignment of the atoms), this representation allows a diagonalization of the relaxation matrix - all relaxation parameters depend on the rank k of the components only. For the case of F_ρ=2, the maximum rank of the polarization moments is k=4, the so-called hexadecapole moment. The modified basic system of equations [17] was specified for the atomic transition F_f=1→F_φ=2 and the experimental geometry. The quantization axis was chosen parallel to the electric vector $\boldsymbol{E}(\equiv E_z)$ of the laser field (Fig. 2). The scanned magnetic field $\boldsymbol{B}_{scan}(\equiv \boldsymbol{B}_x)$ is perpendicular to this axis. An additional arbitrary oriented magnetic field $\boldsymbol{B}$ was included for description of the influence of stray magnetic field on the CPT resonances.

Using a rotating wave approximation and assuming a single-frequency laser field, i.e.

$$\boldsymbol{E_Q}(\omega_L, t) = \boldsymbol{e}_Q \cdot E \cdot exp\{-i(\omega_L t - ks)\} + c.c., \qquad (2)$$

$\boldsymbol{e}_Q$ - circular components of the laser field, the system of equations was reduced to an algebraic one. The obtained system of equations was solved numerically to study the solution dependence on a set of parameters: Rabi frequency ($\Omega_R = d \cdot E/h$), the widths of the levels f and φ, the spontaneous emission transfer coefficients $\Gamma_{f\varphi}(k)$ and the stray field components B_y, B_z. All these parameters and the magnetic fields are expressed in units $\gamma_f(0)$, which denotes the upper level (f) population decay constant. The initial (without laser field broadening) low level population relaxation rate constant $\gamma_\varphi(0)$, was determined by the time of flight for the atoms ($\gamma_\varphi(0) \sim 0.001\ \gamma_f(0)$). We also assumed all rate constants $\gamma_\rho(k)$ for the tensor components ρ_q^k to be equal. The very recent experiments [18] give for the ratio $\gamma_\varphi(2)/\gamma_\varphi(4)$ a value in the interval 0.7-0.9 for different powers of excitation. In the model used, the transversal alignment of the upper level is neglected. This is why in the presentation below the indices k in the designation of the decay constants $\gamma_\rho(k)$ will be omitted.

In a dipole approximation, the spontaneous emission intensity and absorption are defined only by the tensor components ρ_q^k with rank $\kappa \leq 2$. The unpolarized fluorescence intensity $I_{f\varphi}^{unpol}$ can be written as [17,19]:

$$I_{f\varphi}^{unpol} = C_0[\frac{f_0^0}{\sqrt{2F_f+1}} + (-1)^{F_f+F_\varphi+1}\sqrt{30}\begin{Bmatrix} 1 & 1 & 2 \\ F_f & F_f & F_\varphi \end{Bmatrix} f_0^2] \quad (3)$$

Only the two tensor components for the upper level - f_0^0 and f_0^2 describe the signal observed in this case. In linear approximation, both components do not depend on the magnetic field. The magnetic field dependence is the result of the transfer of coherence created on the low level and it is a typical nonlinear effect. In a strong laser field, both these components will be influenced by the hexadecapole components of the ground state. This is why in our numerical calculations we focused our attention on the f_0^0 and f_0^2 tensor components, as well as on the high rank (HR) coherences (octupole ξ_0^3 and hexadecapole φ_q^4) related to the ground state. The main part of the unpolarized intensity is determined by the upper level population f_0^0 (Fig. 6). The influence of the longitudinal alignment f_0^2 on the shape is mainly on the wings of the curve [20].

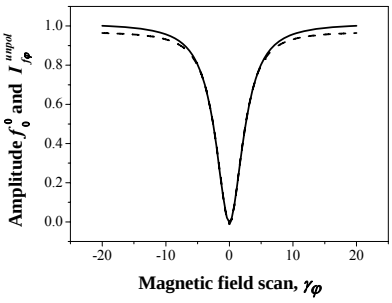

Fig. 6. Comparison of the upper level population f_0^0 (solid line) and the unpolarized intensity $I_{f\varphi}^{unpol}$ (dashed line).

Theoretical analysis of the shapes, amplitudes and widths of the resonances observed in this experimental system at low laser power density (~0.05 mW/cm^2) was performed in [11]. The results were in good agreement with the experimental, although the velocity distribution of the atoms was not included.

In our recent works [20,21], in contrast to the previously considered case of atoms at rest [11,22,23], the Maxwell velocity distribution of the atoms is taken into account. The solution for a given variable ρ_q^k is taken after summarizing the partial solutions for the sub-ensemble of atoms with velocities in a given interval. The integration step and the integration region were varied.

The developed theoretical model describes well the power dependence of the shape of the broad structure, as well as the influence of stray magnetic fields on the resonances. The model does not include the narrow structure and the width narrowing in strong laser fields.

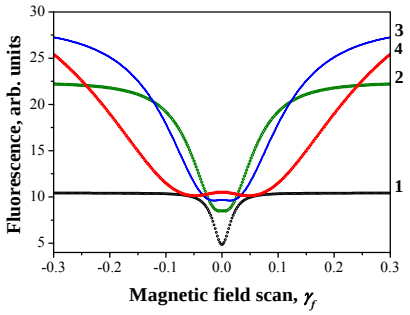

Fig. 7. Calculated shape of the CPT resonances at different Rabi frequencies Ω_R: curve (1) $\Omega_R = \gamma_f$; (2) $\Omega_R = 3\gamma_f$; (3) $\Omega_R = 5\gamma_f$; (4) $\Omega_R = 10\gamma_f$.

On Fig. 7 the calculated shape of the CPT resonances at different Rabi frequencies Ω_R is presented. At relatively low power (curve 1) the shape is close to Lorentzian. The calculated difference between the theoretical shape and its Lorentzian fit is presented on Fig. 8. This structure is in good agreement with the obtained from the experiment [21,24].

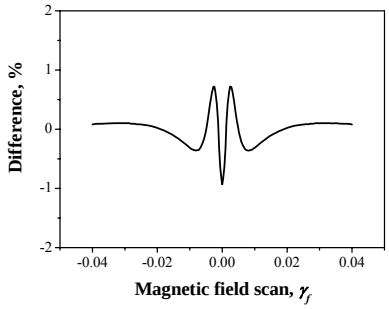

Fig. 8. Difference between calculated resonance shape and its Lorentzian profile fit at Ω_R=1 MHz (~0.2γ_f).

Increasing the pumping power the resonance broadens, flattens and an inverse narrow structure appears at zero magnetic field (Fig. 7, curves 2-4). In our experiments, we cannot directly observe the inverse resonance, because it is with opposite sign of the sign of the narrow structure. The influence of the HRPM on the shape of the single frequency CPT resonances is investigated in details in [21].

The influence of stray magnetic fields on the CPT resonances is very important for precise magnetic field measurements. In the general case, the presence of an additional arbitrarily oriented magnetic field cancels the axial symmetry leading to the appearance of tensor components, which are characteristic of the bi-axial alignment. For example, the non-zero components *Re* φ_1^2,

Im φ_2^2, *Im* φ_2^4, *Im* φ_4^4 appear. As it was pointed in [25], the hexadecapole moment converts into different polarization moments of rank $\kappa \leq 2$. In order to demonstrate the relation between the stray magnetic field and that conversion, we made comparative numerical simulations taking also into account the atoms' velocity distribution [20]. We investigated the influence of small stray magnetic fields B_y and B_z $[B_y \sim (1 \div 10) \cdot \gamma_\varphi(0), B_z \sim (1 \div 50) \cdot \gamma_\varphi(0)]$ on the hexadecapole (φ_q^4), on the octupole (ξ_0^3) and on the observable quadrupole (f_0^2) components. As in the case of atoms at rest [22], the widths of the components with rank $k=4$ as a function of the scanned magnetic field are about twice as small as those of the corresponding quadrupole ($k=2$) resonances and they are more sensitive to magnetic fields. In the cases when the narrow structure of the CPT resonance is suppressed, these components can be observed using polarization or frequency discrimination [26] in the detection of the spontaneous emission or absorption. In this way, the sensitivity of the magnetic field measurements will be increased.

A way for elimination of the narrow structure of the resonance is applying a small transverse to the polarization vector and to the propagation direction magnetic field B_y [10]. In Fig. 9 the CPT signals measured at different magnetic fields B_y [21] are given. The comparison of the central regions of the resonances observed at B_y=0 (curve 1) and at B_y=32 mG (curve 2) shows that at this power density the amplitude of the CPT resonance in a magnetic field is reduced twice and an additional inverted structure (about 5% in amplitude) appears. At higher magnetic fields, this inverted structure disappears (curve 3). The theoretical shape changes of a CPT resonance at different transverse magnetic fields repeat in general the shape changes of the experimental profiles [21].

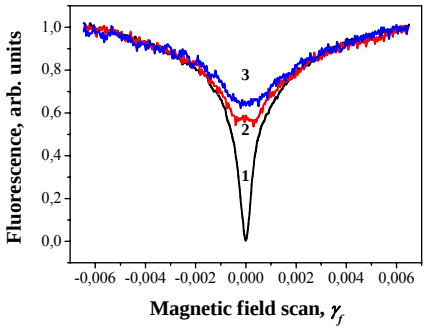

Fig. 9. CPT signals at different magnetic fields B_y transverse to the polarization vector and to the propagation direction: curve (1) B_y = 0 mG; (2) B_y=32 mG; (3) B_y=72 mG.

5. Method for magnetic field measurements

The method for magnetic field measurements based on the single frequency CPT resonances is described in [27,28]. Additional magnetic field $\boldsymbol{B_x}$ parallel to the direction of scanning does not change the resonance shape.

As the CPT resonance is observed at zero magnetic field, $\boldsymbol{B_x}$ only changes the position of the resonance on the scanning magnetic field $\boldsymbol{B_{scan}}$ scale. The difference between the zero of the scanned magnetic field and resonance position gives the value and the sign of the magnetic field component (Fig. 10). The dependence on the resonance position on magnetic field collinear to the scanned one is linear. At strong magnetic fields the method is not limited by the resonance width. The precision of magnetic field determination depends on the precision of determining the resonance maximum on the magnetic scale. In order to increase it and the signal to noise ratio as well, the first derivative of the dark resonance is detected. The scanned magnetic field has two components- slow scanning component and the modulation AC component. The first derivative of the fluorescence signal is measured by a lock-in amplifier referenced to the modulation frequency of the magnetic field.

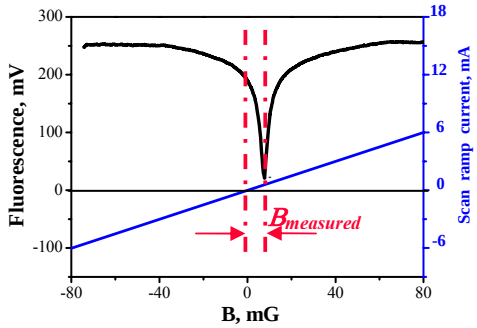

Fig. 10. Principle of magnetic field measurements.

The sensitivity ε of the method is determined by the resonance width ΔB and signal to noise ratio S/N as:

$$\varepsilon = 0.5\ \Delta B/(S/N). \quad (4)$$

When the narrow component of CPT resonance registered in uncovered vacuum cell is used for magnetic field measurements, we are increasing the sensitivity in two ways: 1/ the narrow structure width is about 2 orders narrower than the broad one and 2/ the narrow structure is not power broadened and working at high powers we can increase the S/N ratio. The main source of noise is the electronics.

To test the system in real conditions the Rb cell was placed in a cube with 6 pairs of Helmholtz coils- 3 for magnetic field scanning and 3 for compensation of laboratory magnetic field in the 3 directions. Laboratory magnetic field was compensated by switching sequentially the scanned magnetic field in the 3 orthogonal directions. The component of the magnetic field in each direction was determined by the position of CPT resonance and compensated by applying the suitable current through the second coil. After the compensation the width of the narrow structure of the resonance was 2 mG. To evaluate

the sensitivity of the set-up to small magnetic fields we fixed B_{scan} at zero value, corresponding to the maximum slope of the dispersion curve of the resonance. The sensitivity of the set-up was tested by applying on the sweeping coils square pulses of current corresponding to a given variation δB (from ΔB/2 to the smallest detectable value). The frequency of the current pulses was 0.5 Hz. In our experiment, a typical signal to noise ratio 1200 was measured. The sensitivity of the system for weak magnetic field detection was evaluated to be 1 μG.

5. Conclusions

The investigation of the single frequency CPT resonances in uncoated vacuum cell has shown that the resonance has a complex shape – a narrow structure superimposed on a broader one.

In the cases where narrow signals and high signal-to-noise ratios are needed, the narrow structure of the CPT resonance measured in fluorescence offers the best possibilities: it is not power broadened; its width does not depend on the position of the detector and its amplitude increases with the power.

In the cases where the amplitude of the narrow structure in the CPT resonances is small, or for measurement of strong magnetic field, the wide structure of the CPT resonance at high laser power densities can be used for magnetic field measurements. The sensitivity of the magnetic field measurements can be increased by observation of the HRPM components. The proposed methodology for measurement of strong magnetic fields is not limited by the width of the resonance.

The numerical simulations based on density matrix formalism, which take into account the HRPM influence and the velocity distribution of the atoms show that the HRPM influence the shape at all powers and this influence can be used for explanation of the observed CPT resonance shape peculiarities at the center of the resonance.

The performed experimental and theoretical investigations show that the single frequency CPT resonances have potential for building simplified systems for precise magnetic field vector components compensation and measurement.

Acknowledgements

The authors are pleased to acknowledge the financial support of the European Community (Project G6RD-CT-2001-00642) and the National Science Fund of Republic of Bulgaria (Grant F-1409/04).

References

[1] I. K. Kominis, T. W. Kornack, J. C. Allred, M. V. Romalis, Nature **422**, 596 (2003).
[2] S. Knappe, P. D. D. Schwindt, V. Gerginov, V. Shah, L. Liew, J. Moreland, H. G. Robinson, L. Hollberg, J. Kitching, J. Opt. A: Pure Appl. Opt **8**, S318 (2006).
[3] D. Budker, M. Romalis, Nature Physics **3**, 227 (2007).
[4] E. B. Alexandrov, M. Auzinsh, D. Budker, D. F. Kimball, S. M. Rochester, V. V. Yaschuk, J. Opt. Soc. Am. B **22**, 7 (2005).
[5] D. Budker, W. Gawlik, D. F. Kimball, S. M. Rochester, V. V. Yashchuk, A. Weis, Rev. Mod. Phys. **74**, 1153 (2002).
[6] E. Arimondo, Prog. Opt. **35**, 257 (1996).
[7] R. Wynands, A. Nagel, Appl. Phys. B **68**, 1 (1999).
[8] G. Alzetta, A.Gozzini, L. Moi, G. Orriols, Nuovo Cimento **36**, 5 (1976).
[9] Y. Dancheva, G. Alzetta, S. Cartaleva, M. Taslakov, Ch. Andreeva, Opt. Commun. **178**, 103 (2000).
[10] E. Alipieva, S. Gateva, E. Taskova, S. Cartaleva, Opt. Lett. **28**(19), 1817 (2003).
[11] A. Huss, R. Lammegger, L. Windholz, E. Alipieva, S. Gateva, L. Petrov, E. Taskova, G. Todorov, JOSA B **23**(9), 1729 (2006).
[12] A. Godone, F. Levi, S. Micalizio, J. Vanier, Eur. Phys. J. **D18**, 5 (2002).
[13] A. Corney, Atomic and Laser Spectroscopy, Clarendon Press, Oxford (1977).
[14] F. Levi, A. Godone, J. Vanier, S. Micalizio, G. Modugno, Eur. Phys. J. **D12**, 53 (2000).
[15] S. Gateva, E. Alipieva, E. Taskova, Phys. Rev. A **72**, 025805 (2005).
[16] B. Decomps, M. Dumont, M. Ducloy, in Laser Spectroscopy of Atoms and Molecules, edited by H. Walther, Springer-Verlag, Berlin Heidelberg New York, (1976).
[17] M. I. D'yakonov, V. I. Perel, Optics and Spectroscopy **20**, 101 (1966).
[18] S. Pustelny, W. Lewoczko, W. Gawlik, Phys. Rev. A **73**, 023817 (2006).
[19] E. B. Alexandrov, M. P. Chaika, G. I. Hvostenko, Interference of Atomic States, Springer-Verlag (1991).
[20] L. Petrov, D. Slavov, V.Arsov, V. Domelunksen, V. Polischuk, G. Todorov, Proc. SPIE 6604, 66040H (2007).
[21] S. Gateva, L. Petrov, E. Alipieva, G. Todorov (unpublished)
[22] G. Todorov, L. Petrov, D. Slavov, V. Polischuk, M. P. Chaika, Proc. SPIE **5449**, 380 (2003).
[23] V. Polischuk, L. Petrov, D. Slavov, V. Domelunksen, G. Todorov, Proc. SPIE **6257**, 62570A (2006).
[24] E. Pfleghaar, J. Wurster, S.I. Kanorsky, A. Weis, Opt. Commun. **99**, 3003 (1993).
[25] A. I. Okunevich, Opt. Spectrosc. **91**(2), 177 (2001).
[26] E. Alipieva, S. Gateva, E. Taskova, Proc. SPIE **6604**, 66040G (2007).
[27] E. Alipieva, S. Gateva, E. Taskova, IEEE Trans. Instr. Meas. **54**(2), (2005).
[28] E. Alipieva, C. Andreeva, L. Avramov, G. Bevilaqua, V. Biancalana, E. Borisova, E. Breschi, S. Cartaleva, Y. Dancheva, S. Gateva, T. Karaulanov, R. Lammegger, L. Moi, L. Petrov, N. Petrov, D. Slavov, E. Taskova, G. Todorov, L. Windholz, A. Yanev, Proc. SPIE **5830**, 170-175 (2005).

*Corresponding author: sgateva@ie.bas.bg